Article ID: 1006-8775(2019) 01-0045-09

# DIURNAL VARIATION OF GLOBAL PRECIPITATION: AN ANALYSIS OF CMORPH DATA

XING Shu-qiang (邢书强), LI Xiao-fan (李小凡)
(Department of Atmospheric Sciences, School of Earth Sciences, Zhejiang University, Hangzhou 310027 China)

**Abstract:** In this study, the observed CMORPH precipitation data from 1998 to 2015 are used to analyze diurnal variation of global precipitation. The results reveal that the strong diurnal signals of precipitation occur over equatorial continental areas where the annual precipitation centers are located. The phase of diurnal variation of global precipitation reveals a distinct land-sea contrast with nocturnal peaks at sea and afternoon maxima over continents. The analysis of six selected area reveals that precipitation peak over equatorial land areas occur in afternoon and maximum diurnal signals appear in autumn or winter. Eastern equatorial Intertropical Convergence Zone (ITCZ) barely shows diurnal signals in the entire year. Precipitation over Sichuan Basin and northwestern Pacific shows nocturnal peak and the maximum diurnal amplitude in summer. Precipitation over coastal areas off eastern China shows an afternoon peak and the largest diurnal amplitude in summer.

**Key words:** global precipitation, diurnal variation, CMORPH data, seasonal impact
**CLC number:** P426.62.3 **Document code:** A
doi: 10.16555/j.1006-8775.2019.01.005

## 1 INTRODUCTION

Diurnal variation is one of the most fundamental cycles of the Earth's climate system, which stems from the solar radiation. Over 100 years ago, Kincer found that the peak of precipitation in many stations in the central United States mostly occurred at night, while the precipitation in the southeastern coast of the United States had an afternoon peak[1]. Kikuchi and Wang analyzed precipitation data from tropical marine areas collected from nine weather ships and showed a peak of precipitation at night [2]. Due to the limitation of data, the early studies on the diurnal variation of precipitation are mostly limited to local areas or limited periods, so it is difficult to conduct a comprehensive and systematic study of diurnal variation of precipitation (Yu et al.[3]). Until recent years, with the improvement of the meteorological observation station network and the extensive application of radar and satellite in the weather as well as and the numerical model, data with high temporal resolution is more readily available, making remarkable progresses of the studies of diurnal variation of precipitation.

Because of the difference of the nature of the underlying surface, the diurnal variation of precipitation shows regional characteristics. Wang et al. studied the diurnal variation of precipitation in southwestern China by using the hourly precipitation data from observation stations[4]. They showed that precipitation in the southwestern region is mainly characterized by the main peak in the early morning and the second peak in the afternoon. Tang et al. studied the seasonal variation of diurnal variation of precipitation in southwestern China[5]. They found that nighttime rainfall is dominant in Sichuan, Chongqing and Guizhou, while daytime precipitation is dominant in Yunnan. Precipitation in Chongqing occurred mostly in the early morning to noon in autumn, winter and spring. In contrast, in summer, precipitation in the southeast Chongqing occurs frequently in the afternoon.

When studying the diurnal variation of summer precipitation in China, Yu et al. selected five representative regions base on the phase and trend of diurnal variation of diurnal precipitation. They are eastern side of Tibet Plateau and Sichuan Basin, the middle reaches of the Yangtze River, Southeast China, Northeast China, Central and East China[6]. Li et al. also analyzed the seasonal variation of the diurnal cycle of precipitation in southern China [7]. They found that during summertime precipitation appears in the night and early morning over southwest region whereas it occurs in the afternoon over southeast region. During wintertime, a peak of precipitation shows from midnight to early morning over entire southern region.

Huang et al. used the precipitation data retrieved from TRMM 3B42 from 1998 to 2010 to study the diurnal variation of China precipitation in summer and autumn [8]. They showed that in summer, precipitation appears from afternoon to evening in most parts of China. However, in some areas of the Yunnan-Guizhou Plateau, Sichuan Basin and Tibet Plateau, the precipitation reaches

**Received** 2018-01-18; **Revised** 2018-11-26; **Accepted** 2019-02-15
**Foundation item:** National Natural Science Foundation of China (41775040, 41475039); National Key Basic Research and Development Project of China (2015CB953601)
**Biography:** LI Xiao-fan, Ph.D., Professor, primarily undertaking research on mesoscale meteorology, cloud microphysics.
**Corresponding author:** LI Xiao-fan, e-mail: xiaofanli@zju.edu.cn

peak in early morning. The precipitation with a maximum from late night to early morning is extended to the central Qinghai-Tibet Plateau, the Yunnan-Guizhou Plateau and the northwestern China in autumn. By using data from TRMM 3B42, Mao and Wu studied the diurnal variation of summer precipitation over the Asian monsoon region[9]. They found that in the western Pacific ITCZ, the precipitation during daytime is lower than that during nighttime, while in the opposite occurs over the other oceans. In the mainland, eastern China had more frequent precipitation during the day than at night, while the central Indian and Indochina show more frequent precipitation at night than during the day. Precipitation over the mainland usually is in the afternoon, while precipitation appears in evening over central Indo-China Peninsula and central India. The peak of precipitation over the oceans generally appears from midnight to early morning, but precipitation maximum postponed to morning in the South China Sea, the Bay of Bengal and the Arabian Sea. Their results are consistent with those from Lu and Xu [10]. Pinker et al. conducted a study on the precipitation in the sub-Saharan region and found that rainfall often occurred in the evening, with two peaks in the evening (18:00-20:00 LST) and at the midnight (00:00-01:00 LST)[11]. Kikuchi and Wang analyzed the diurnal variations of precipitation in the global tropical oceans[2]. Marine areas are characterized by medium amplitude and early morning peaks (06:00-09:00 LST). The continent is characterized by large amplitude and afternoon peaks (15:00-18:00 LST). Chen et al. analyzed precipitation over the Great Plains and found that short-term rainfall events (events that last in 1 hour) occur more frequently in summer than in the other seasons and tend to have two diurnal maximums: the early morning (04:00-06:00 LST) and the afternoon (15:00-17:00 LST) [12]. However, long-term rainfall events (events that last more than 3 hours) contribute more to precipitation, and have peaks from midnight to early morning (00:00-06:00 LST).

Due to the limitation of observational precipitation data, the previous studies of diurnal precipitation cycles focused on localized diurnal signals and their results are less robust. In this study, the global precipitation data developed by Climate Prediction Center morphing technique (CMORPH) are used to analyze diurnal variations of precipitation. The 18-year data allow us to conduct a robust analysis of diurnal cycles of precipitation from a global view. Data and methodologies are briefly discussed in the next section. The results are presented in section 3. The summary and discussions will be given in section 4.

## 2 DATA AND METHODOLOGIES

The data used in this study is global precipitation estimates from CMORPH. CMORPH data was developed by the National Oceanic and Atmospheric Administration (NOAA) Climate Prediction Center (CPC) in the United States. The morphing technique integrates multiple satellite platforms in time and space for interpolation, to produce global high spatiotemporal resolution precipitation products. The basic principle of CMORPH is to use the high-resolution infrared remote sensing data of geostationary satellite to calculate the motion vector of cloud and precipitation system, and then, the instantaneous precipitation distribution inverted by the microwave remote sensing data of the near-Earth satellite is extrapolated in time and space along with the motion vector to finally form a spatially continuous global precipitation distribution. This method has shown great advantage in validating precipitation in Australia (Joyce et al.[13]). Later, deviation correction was made based on land-based observations and Global Precipitation Climatology Program (GPCP) to construct the improved precipitation estimates. The temporal and spatial resolutions are 30 minutes and 8km×8km over 60°S-60°N.

In this study, the CMORPH precipitation estimation product from 1998 to 2015 was used and the 18-year data were calculated by mathematical composite method. To verify the reliability of CMORPH data, the diurnal composites calculated by the CMORPH data and hourly precipitation data of Hangzhou station from 2005 and 2009 to 2015 are compared (the station data before 2005 and in 2006—2008 are not available). Both diurnal composites in Fig.1 show afternoon peaks, while the peak in the CMORPH data lags that in the station data by 1 hour. The second peaks appear in early morning, while the maximum in the CMORPH data leads that in the station data by few hours. The comparison indicates that the CMORPH data fairly present primary peak, and can be used for further analysis of diurnal precipitation. The CMORPH data have been used for validation of the other precipitation data (Cheng et al.[14]) and have applied to the precipitation studies (Zhou et al.[15]).

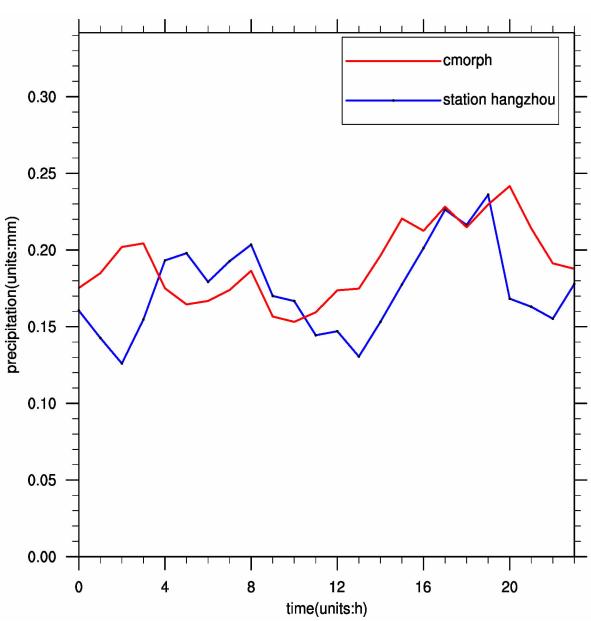


**Figure 1**. The diurnal variations of precipitation of Hangzhou calculated from auto-meteorological station data (blue) and CMORPH data (red).

## 3 RESULTS

The geographical distribution of global average hourly precipitation is shown in Fig.2a. Strong precipitation appears in the tropical continent, the Congo Basin of central Africa and the Amazon Plain of South America. Especially in the east of the Congo Basin, there is a strong precipitation center to the west of the East African Plateau, where the average hourly precipitation is over 0.5 $mmh^{-1}$. Another strong precipitation center appears in the east Pacific coast region to the north of the western Andes of south America. In the tropical Pacific region, the distribution of torrential rainfall areas is relatively regular and basically distributed along the intertropical convergence zone (ITCZ) with an average hourly rainfall of 0.3-0.4 $mmh^{-1}$ and in some area, may exceed 0.5 $mmh^{-1}$. In the Southwest Pacific, heavy precipitation extends from the equator to the southeast arriving to the east of Oceania, whereas in the northwestern Pacific it extends from the equator to the northeast arriving to the east of Japan. This distribution may be related to the warm current. On the other hand, on the both sides of ITCZ, in the area which is affected by the subtropical high all the year round, precipitation was significantly less than the nearby sea area, which the average hourly precipitation below 0.1 $mmh^{-1}$. In the tropical Indian Ocean, the heavy precipitation area extends from equator to the Bay of Bengal, while a clear area of low precipitation is observed near the Tropic of Capricorn. In the tropical Atlantic, except for a strong precipitation region near the equator, both sides are low value area. In addition, the Malayan area is also one of the areas with the highest precipitation in the world, where the average hourly precipitation generally is over 0.3 $mmh^{-1}$. Especially in the northwestern New Guinea islands, the areas with the highest average hourly precipitation in the world were observed, which may be related to the upwelling of the Walker circulation loop here and the northwest-southeast ridge of the island.

Over the north temperate zone, most of inland area shows a low precipitation, except for some sporadic areas such as the Mediterranean Sea, the Black Sea, the Caspian Sea, the Aral Sea, and the Great Lakes in North America, where average hourly precipitation exceeds 0.1 $mmh^{-1}$. The east coast of continent is relatively humid with an average hourly precipitation of over 0.1 $mmh^{-1}$. With the influence of the terrain, strong precipitation occurs in the south and east sides of Tibetan Plateau and the east side of Rocky Mountain. Especially in the Gangers plain, the south side of Tibetan of Plateau, the average hourly precipitation reaches over 0.2 $mmh^{-1}$.

Over the south temperate zone, low precipitation occurs in South Africa, with sporadic areas of relatively high precipitation in valleys and coastal plains, indicating that low precipitation may be associated with high altitude. An average precipitation of greater than 0.1 $mmh^{-1}$ appears only in the north and east of Australia . In South America, however, precipitation in the western region is lower because of the Andes mountain, but the average precipitation in the east is higher than that of the other land areas, which may be related to the terrain and the Brazilian warm current.

To examine precipitation peak within a day, the maximum hourly precipitation over the diurnal variations of global precipitation is shown in Fig.2b. The horizontal distribution of maximum hourly precipitation is similar to that of the average hourly precipitation (Fig.2a), High precipitation is located over the ITCZ. It is worth noting that over the Pacific Ocean, the precipitation maxima extend southward by about 10 latitudes. Several large precipitation centers emerge near the east and south coasts of the Japanese islands. Over the Atlantic Ocean, a precipitation center emerges near the Gulf Stream on the shores of the United States. A precipitation center also appears along the northeastern coast of the Bay of Bengal.

Over the continents, precipitation centers in the Congo Basin, New Guinea and the Pacific to the north of the Western Andes are over 2 $mmh^{-1}$. The precipitation maxima also appear in the Gulf of Guinea, the Gulf of Bengal, the northern and eastern coasts of Australia and the eastern coasts of Asia and America continent, respectively, with the magnitudes of 0.3-0.5 $mmh^{-1}$. Unlike the ocean and coast region, there are several sporadic precipitation centers in the low hourly mean hour precipitation region of inland areas.

Figure 2c shows the amplitude (maximum precipitation minus minimum within a day) of diurnal variations in global precipitation. The large diurnal signals mainly occur in the tropics and subtropics, while in the temperate and high latitudes, the diurnal signals mainly appear in the Mediterranean Sea, the Black Sea, the Aral Sea, Alaska Bay and southwestern coast of South America.

On the tropical oceans, large amplitudes of diurnal precipitation appear in ITCZ region and some islands in the northeastern Australasia exceed 0.1 $mmh^{-1}$. The large diurnal amplitudes are mainly found in the tropical continent, tropical islands and the coast area in the middle and low latitudes. In the Africa, large amplitudes occur in the Gulf of Guinea, the Congo Basin and the west of the Russian Ethiopian Plateau. In Asia, amplitudes in the Indian Peninsula and the Bay of Bengal are over 0.1 $mmh^{-1}$. In addition, Indo-China Peninsula, China's southeast coast and the southwestern side of Japan's Kyushu Island also show large diurnal amplitudes. The diurnal magnitudes in southern Indochina Peninsula are over 0.5 $mm\ h^{-1}$. It is interesting to note that large amplitudes appear over inland areas of southwest China, which may be related to the topographic lifting of the Tibet Plateau. The Malaysia shows the large amplitudes of diurnal precipitation in the world. In America, southern Mexico and the north-eastern Amazon plain have amplitudes of diurnal precipitation of 0.5-0.7 $mmh^{-1}$. The diurnal magnitudes in the Pacific Coast region of

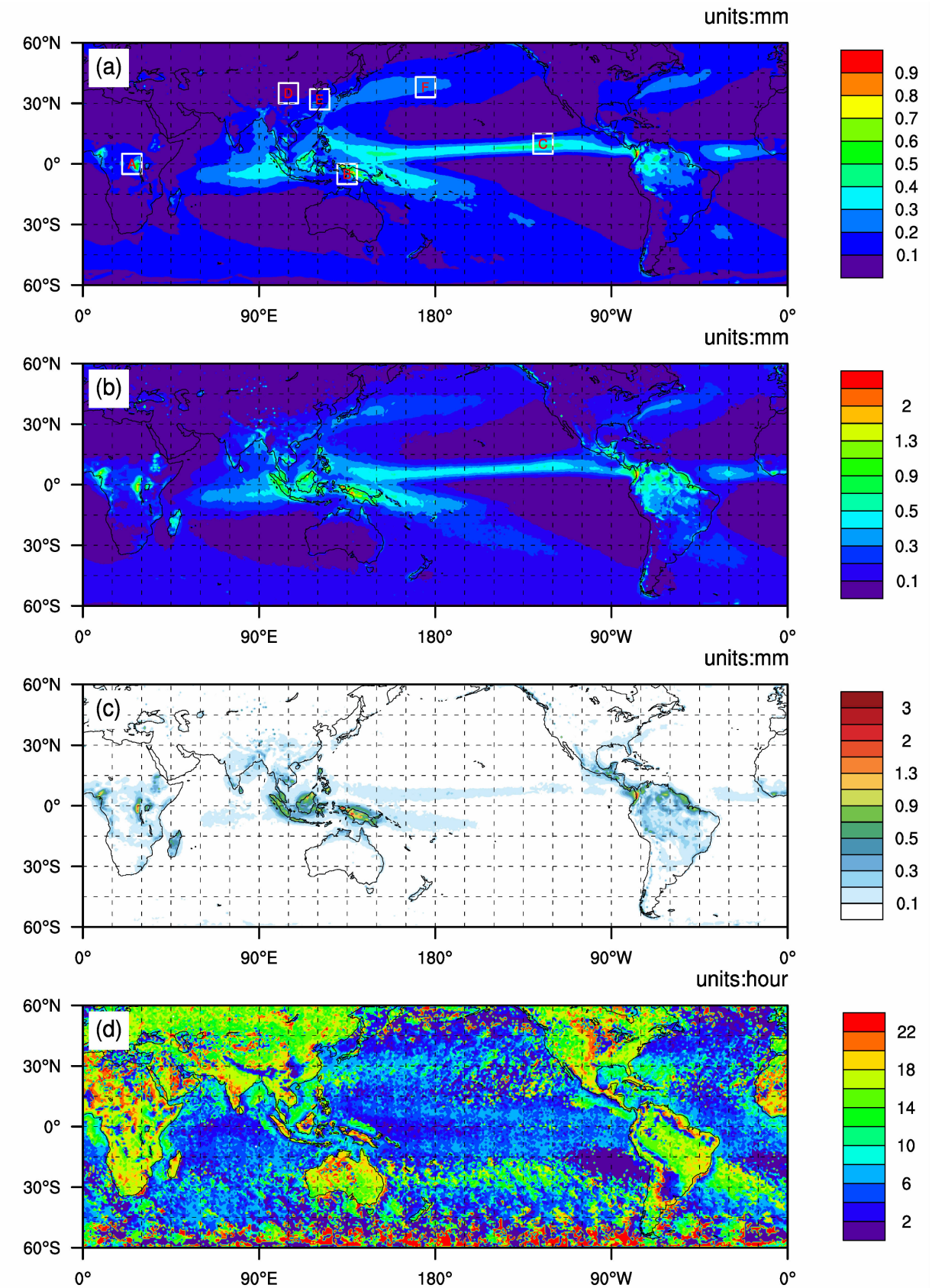


**Figure 2**. Horizontal distribution of (a) time-mean precipitation, (b) maximum precipitation within a day, (c) amplitude and (d) phase of diurnal variation of precipitation. There are six selected areas for further analysis in Fig.2a. A, B, C, D, E and F denote Congo Basin (20-30°E, 5°S-5°N), New Guinea island and its western waters (130-140°E, 10°S-EQ), ITCZ (130-120°W, 5°N-15°N), Sichuan Basin and the Loess Plateau (100-110°E, 30-40°N), coastal areas over east China (116-126°E, 27-37°N) and northwest Pacific (170-180°E, 33-43°N), respectively.

north-western South America are 1.3-1.5 $mmh^{-1}$.

In order to reveal the time when the maximum precipitation appears within a day, Fig.2d shows the phase distribution of global diurnal precipitation. The maximum precipitation generally appears in the early morning (00:00-08:00 LST) over the oceans, and mainly occurs in the afternoon to the evening (14:00-22:00 LST) in the continents. The maximum precipitation occurs in the morning to noon (08:00-14:00 LST) mainly near the continental coast of middle and low latitudes, which is consistent with the result from Kikuchi and Wang [2]. The nocturnal peak of diurnal precipitation over the ocean areas is mainly due to the absence of solar radiation at night; the dominant infrared radiative cooling leads to the falling of local temperature and thus the increase in saturation mixing ratio, increasing condensation and precipitation (Sui et al.[16]; Gao et al.[17]; Gao and Li[18]).

The maximum precipitation occurs in the afternoon (12:00-16:00 LST) in offshore sea areas such as the Gulf of Guinea, the east of the Africa near 10° S, the Bay of Bengal, the eastern and southern seas of China, the northern offshore of New Guinea, the south-central and south-eastern Australian coasts and the southwest offshore of Mexico. This may be due to the development of sea breeze resulting from land-sea contrast during daytime.

The maximum precipitation appears in the early morning of 00:00-06:00 LST over the east and south sides of Tibetan Plateau, of 20:00-04:00 LST over the east side of the Rocky Mountains, the central North America and the north-eastern Amazon of South America, This indicate the dominant effects from nocturnal infrared radiative cooling.

To further analyze the detailed characteristics of diurnal variation of precipitation, six representative areas are selected: A for Congo Basin (20-30°E, 5°S-5°N), B for New Guinea island and its western waters (130-140° E, 10°S-EQ), C for eastern Pacific ITCZ area (130-120° W, 5-15°N), D for Sichuan Basin and the Loess Plateau (100-110° E, 30-40° N), E for East China coastal areas (116-126° E, 27-37° N) and F for Northwest Pacific (170-180°E, 33-43°N). A, B and C represent precipitation centers along the Equator, respectively. D, E and F represent continental, coastal and oceanic areas in the subtropics. The precipitation and its diurnal signals at the north of 40°N are much weaker than those around 30-40°N (D, E and F).

The precipitation of tropical continent (A) and tropical islands (B) has a minimum around 08:00 and a peak around 17:00 LST, while the magnitude of region B is bigger than that of region A (Fig.3a). However, in eastern Pacific ITCZ area (C), the hourly precipitation nearly displays a constant of 0.5 $mmh^{-1}$ all day due to strong large-scale convergence area, indicating no diurnal variation of precipitation there. In temperate regions, on the east side of Plateau (D), precipitation has a peak around 07:00 LST in the morning and a minimum around 21:00 LST in the evening, with the amplitude of about 0.1 $mmh^{-1}$ (Fig.3b). Over the coastal area (E), precipitation has a valley in the morning and a peak in the afternoon, while the diurnal amplitude is less than 0.1 $mmh^{-1}$. In the temperate ocean area (F), precipitation shows a peak around 05:00 LST and a valley around 20:00 LST. The amplitude of diurnal precipitation in the temperate ocean area is smaller than those in the temperate coast (E) and continent area (D), but it is larger than that in eastern Pacific ITCZ area (C).

To examine seasonal change of diurnal variation of precipitation, the diurnal variation of precipitation in all six areas are plotted for spring (March, April and May), summer (June, July and August), autumn (September, October and November) and winter (December, January and February) in Figs.4 and 5. The amplitudes of diurnal variation of precipitation reach maxima in summer, whereas they have minima in winter, when diurnal signals can be neglected.

The maximum precipitation Congo Basin (A) and New Guinea island (B) occurs around 17:00 LST in spring, autumn and winter, whereas it appears around 19:00 LST in summer (Fig.4), indicating seasonal change of diurnal variation of precipitation there. The minimum precipitation in summer also lags that in spring, autumn and winter by 2-3 hours. The precipitation peak in later hours may be associated with warming surface for more conversion from unstable available potential energy to kinetic energy. The precipitation over eastern Pacific ITCZ area (C) area does not show significant diurnal signals all year around due to the location near the equator. The precipitation peaks over Sichuan Basin (D) occur in 04:00-07:00 LST for spring, around 7:00 LST for summer, 08:00 for autumn and 04:00 LST in winter (Fig. 5). The maximum precipitation over East China coastal areas (E) appears around 02:00 LST and 13:00 LST for spring, 16:00 LST for summer, 13:00 LST and 18:00 LST for autumn and 01:00 LST for winter. The precipitation over Northwest Pacific (F) shows peaks around 03:00-07:00 LST and 12:00 LST for spring, 02:00 LST for summer, 05:00 LST, 10:00 LST and 15:00 LST for autumn and 06:00 LST and 21:00 LST for winter. The nocturnal precipitation peak may be related to the decrease in saturation mixing ratio and increase in relative humidity caused by the infrared radiative cooling and the daytime maximum precipitation may be associated with the development of convection caused by the solar radiative heating-induced release of unstable energy.

## 4 SUMMARY AND DISCUSSIONS

In this study, we use CMORPH precipitation data from 1998 to 2015 to analyze the diurnal variation of precipitation in a global view. The results show that precipitation peaks occur in early morning over oceans, whereas they appear in afternoons over continent. The strong diurnal signals of precipitation also occur over the

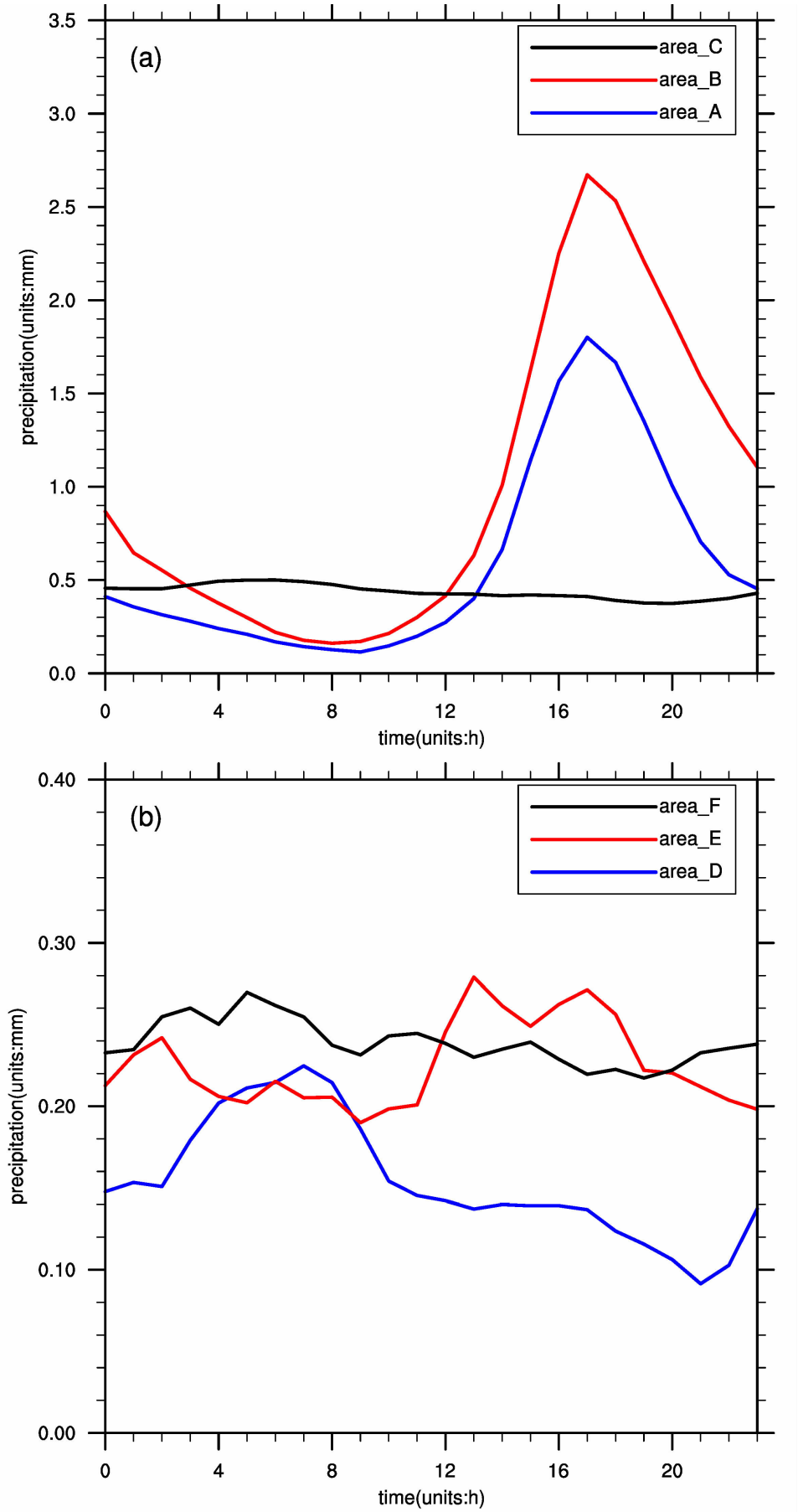


**Figure 3**. Diurnal composites of precipitation for six areas shown in Fig.1a, which are calculated using CMORPH data over the entire years.

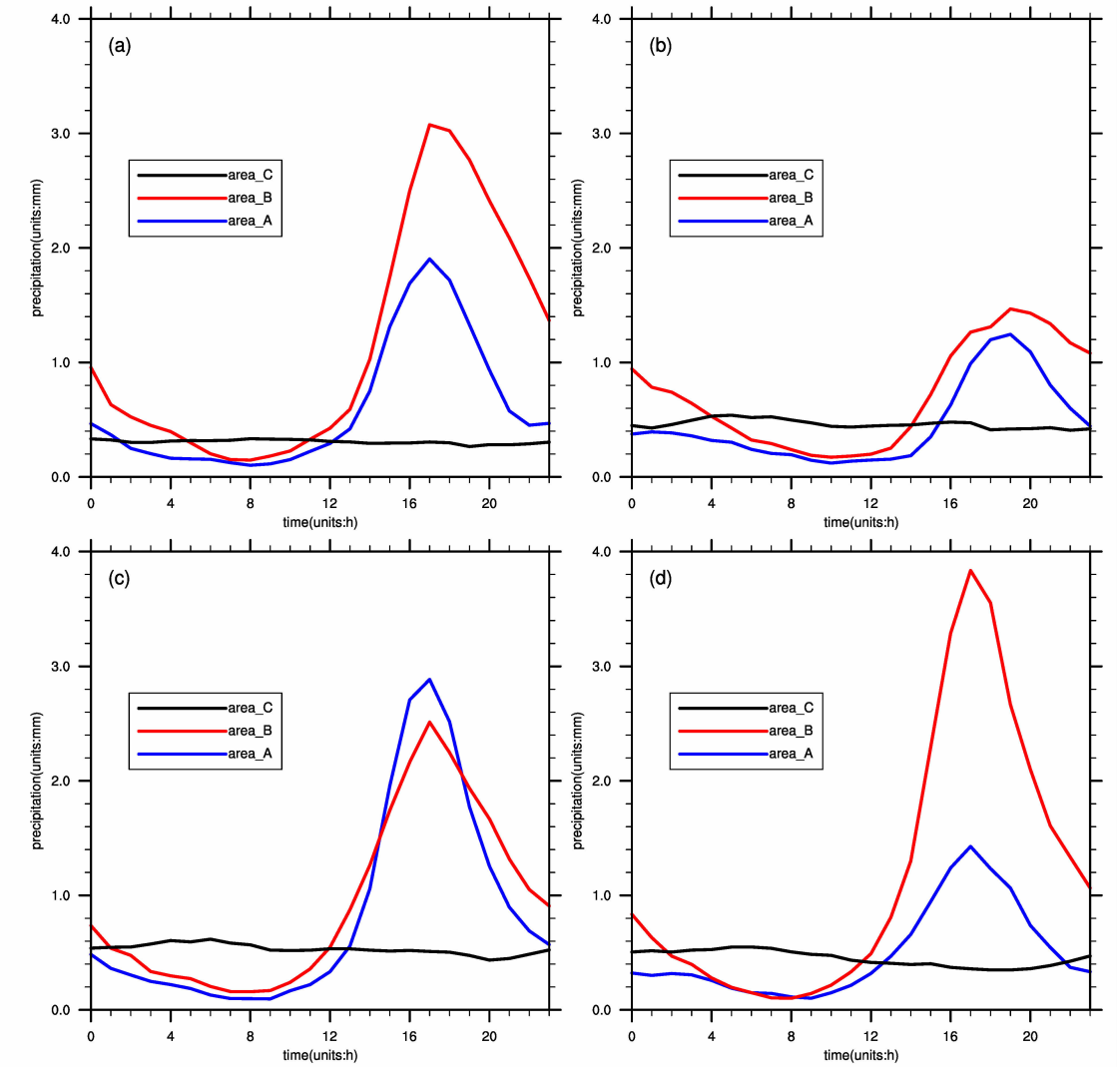


**Figure 4**. Diurnal composites of precipitation in areas A, B and C shown in Fig.1a, which are calculated using CMORPH data in (a) spring, (b) summer, (c) autumn and (d) winter.

Congo Basin, the Malay Archipelago, the Amazon Plain in South America, the central Africa, the Malay Archipelago, and northern South America. The relatively larger amplitudes also appear in the Indian Peninsula and the Bay of Bengal, the eastern and southern sides of the Tibetan Plateau, the eastern coast of China, the Indochina Peninsula, the northern part of Australia and some inland lakes in the Eurasian continent. The amplitudes of daily variation of the ocean area are generally small, but the relatively larger amplitudes occur in ITCZ and oceanic islands.

The horizontal distribution of phase of global diurnal precipitation shows significant land-sea contrast. Generally, the maximum oceanic precipitation within a day appears in the early morning, whereas the continental precipitation peak occurs in the afternoon to evening. In coastal and offshore areas such as the Gulf of Guinea, the Bay of Bengal, the East China Sea and the South China Sea, the maximum precipitation occurs in afternoon. On eastern and southern Tibet Plateau and eastern Rocky Mountains, maximum precipitation occurs from midnight to early morning.

The diurnal variations of precipitation are computed in spring, summer, autumn and winter over six selected areas to study seasonal changes in diurnal signals of precipitation. Congo Basin and New Guinea islands show precipitation peaks in the late afternoon, but diurnal amplitudes reach their peaks in autumn over Congo basin and in winter over New Guinea islands. Since afternoon precipitation peaks often result from the release of unstable energy with the surface warming caused by solar radiative heating, large-scale circulations there may be favorable for development of instability. The diurnal signals are rather weak all year around over eastern Pacific ITCZ. Since ITCZ has strong precipitation all year around, much less solar radiation can go through deep clouds to develop instability in the lower troposphere. The deep clouds do not allow infrared radiation going out to space and maintain warm temperature during nighttime. Precipitation over Sichuan Basin shows nocturnal peak

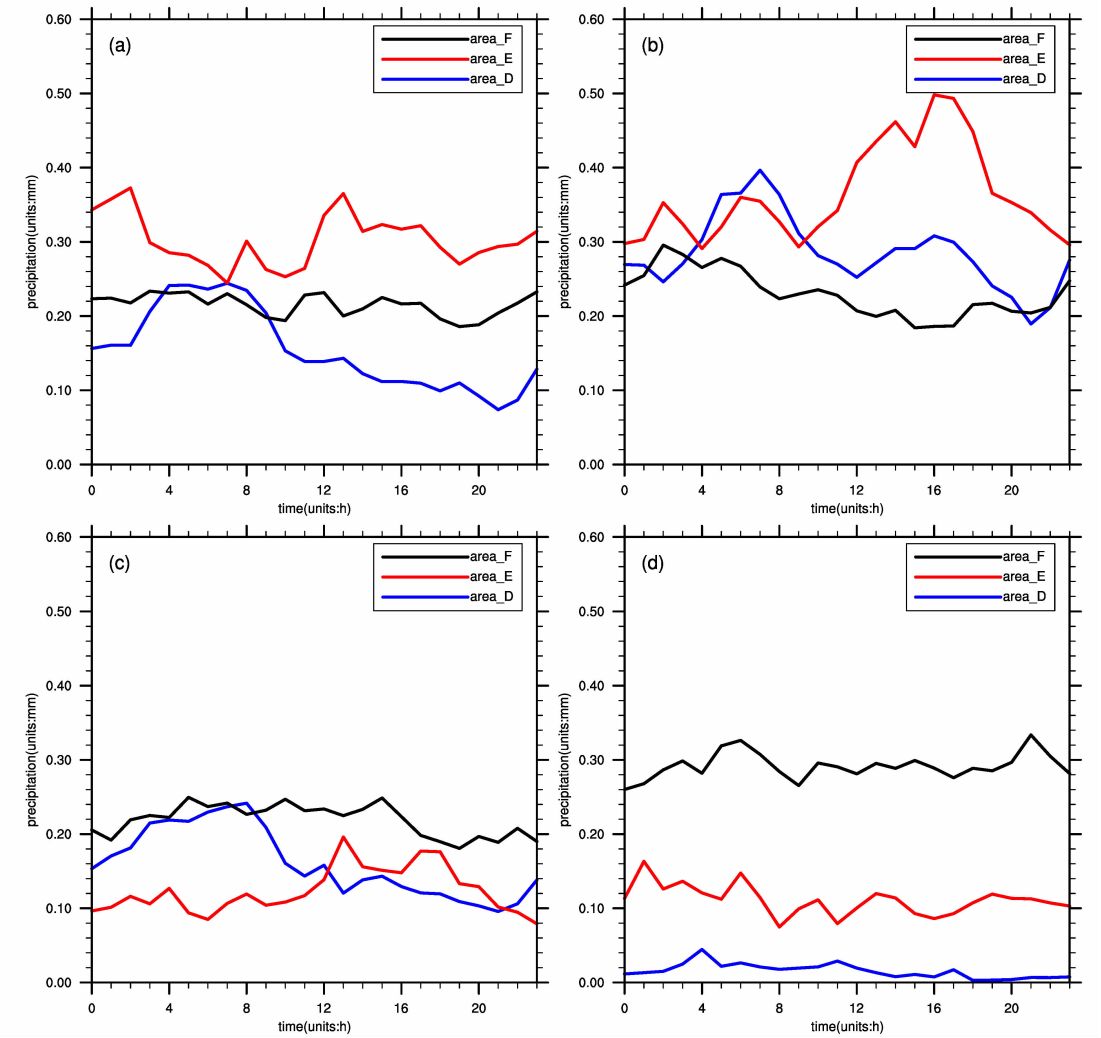


**Figure 5**. As in Fig. 4 except for those in areas D, E and F shown in Fig.1a.

and the maximum diurnal amplitude in summer. Northwestern Pacific along storm tracks has nocturnal peak and the strongest diurnal amplitude in summer. Nocturnal precipitation peak is often associated with the decrease in saturation mixing ratio as a result of nocturnal infrared radiative cooling and increased water vapor during summertime. Precipitation over coastal areas off eastern China shows an afternoon peak and the largest diurnal amplitude in summer, which may be associated with the strong development of sea breeze during summertime.

***Acknowledgement:*** The authors thank the support from the Training Center of Atmospheric Sciences of Zhejiang University.

## REFERENCES:

[1] KINCER J B. Daytime and nighttime precipitation and their economic significance [J]. Mon Wea Rev, 1916, 44 (11): 628-633.

[2] KIKUCHI K, WANG B. Diurnal Precipitation Regimes in the Global Tropics [J]. J Climate, 2008, 21 (11): 2680-2696.

[3] YU Ru-cong, LI Jian, CHEN Hao-ming, et al. Progress in studies of the precipitation diurnal variation over contiguous China [J]. Acta Meteor Sin, 2014, 72 (5): 948-968 (in Chinese).

[4] WANG Fu-chang, YU Ru-cong, CHEN Hao-ming, et al. The characteristics of rainfall diurnal variation over the southwestern China [J]. Torrent Rain Disast, 2011, 30(2): 117-121 (in Chinese).

[5] TANG Hong-yu, GU Jian-feng, YU Sheng-bin, et al. Analysis on diurnal variation of precipitation in southwest China [J]. Plateau Meteor, 2011, 30(2): 376-384 (in Chinese).

[6] YU R, ZHOU T, XIONG A, et al. Diurnal variations of summer precipitation over contiguous China [J]. Geophys Res Lett, 2007, 34(1): 223-234.

[7] LI J, YU R, ZHOU T. Seasonal variation of the diurnal cycle of rainfall in the southern contiguous China [J]. J Climate, 2008, 21(22): 6036-6043.

[8] HUANG Tian-fu, XIE Jia-jun, LIU Peng. Precipitation diurnal variations of the summer and autumn based on multi-national satellite data [J]. Guizhou Meteor, 2013, 37 (6): 30-33 (in Chinese).

[9] MAO Jiang-yu, WU Guo-xiong. Diurnal variations of summer precipitation over the Asian monsoon region as revealed by TRMM satellite data [J]. Sci China Earth Sci,

2012, 55(4): 554-566.
[10] LV Xiong, XU Hai-ming. Diurnal variations of rainfall in summer over the Indo-China Peninsula [J]. J Nanjing Inst Meteor, 2007, 30(5): 632-642 (in Chinese).
[11] PINKER R T , ZHAO Y, AKOSHILE C, et al. Diurnal and seasonal variability of rainfall in the sub-Sahel as seen from observations, satellites and a numerical model [J]. Geophys Res Lett, 2006, 33(7): 359-377.
[12] CHEN H, ZHOU T, YU R, et al. Summer rainfall duration and its diurnal cycle over the US Great Plains [J]. Int J Climatol, 2009, 29(10): 1515-1519.
[13] JOYCE R J, JANOWIAK J E, ARKIN P A, et al. CMORPH: A method that produces global precipitation estimates from passive microwave and infrared data at high spatial and temporal resolution [J]. J Hydrometeor, 2004, 5(3): 287-296.
[14] CHENG Lu, SHEN Runping, SHI Chunxiang, et al. Evaluation and verification of CMORPH and TRMM 3B42 precipitation estimation produces [J]. Meteor Mon, 2014, 40(11): 1372-1379 (in Chinese).
[15] ZHOU Xuan, LUO Ya-li, GUO Xue-liang. Application of a CMORPH-AWS merged hourly gridded precipitation product in analyzing characteristics of short-duration heavy rainfall over southern China [J]. J Trop Meteor, 2015, 31(3): 333-344 (in Chinese).
[16] SUI C H, LI X, LAU K M. Radiative-convective processes in simulated diurnal variations of tropical oceanic convection [J]. J Atmos Sci, 1998, 55 (13): 2345-2357.
[17] GAO Shou-ting, CUI Xiao-peng, LI Xiao-fan. A modeling study of diurnal rainfall variations during the 21-day period of TOGA COARE [J]. Adv Atmos Sci, 2009, 26 (5): 895-905.
[18] GAO S, LI X, Precipitation equations and their applications to the analysis of diurnal variation of tropical oceanic rainfall [J]. J Geophys Res, 2010, 115, D08204, doi: 10.1029/2009JD012452.

**Citation:** XING Shu-qiang and LI Xiao-fan. Diurnal variation of global precipitation: An analysis of CMORPH data [J]. J Trop Meteor, 2019, 25(1): 45-53.